TRANSPORT PROPERTIES OF POLYCRYSTALLINE NbB$_3$Sn FILMS ON SAPPHIRE SUBSTRATES

M. Perpeet[1], W. Diete[1,2], M. A. Hein[1], S. Hensen[1], T. Kaiser[1], G. Müller[1], H. Piel[1], J. Pouryamout[1]

[1] FB Physik, Universität Wuppertal, Gaußstr. 20 , D-42097 Wuppertal, Germany
[2] ACCEL Instruments GmbH, D-51429 Bergisch-Gladbach, Germany

Abstract. Nb$_3$Sn films on low-loss dielectric substrates are interesting for comparison with the transport properties and field limitations of other superconducting films, especially in microwave applications. We have prepared polycrystalline Nb$_3$Sn films on sapphire by a combination of two well-approved processes. Nb precursor films are DC-magnetron-sputtered onto the substrates and afterwards converted into Nb$_3$Sn by Sn-vapour diffusion at 1150°C. The process allows to control the grain size by converting Nb-precursors of different thickness (grain size $\cong$ film thickness $\leq$ 3μm). For films thicker than 1μm, the transport properties were comparable to high-quality Nb$_3$Sn layers on bulk Nb.

The critical temperature and the current density were T = 18.0K, $\Delta T_c \leq$ 0.2K and j_c(4.2K) $\leq$ 8MA/cm^2. At 4.2K the temperature dependent surface resistance R_s(T) at 19 (87)GHz dropped below the sensitivity limit of the measurement systems of 20 (500)μΩ (i. e. 50nΩ @ 1GHz, $R_s \propto f^2$). R (T) revealed an energy gap $\Delta/kT_c \leq$ 2.3, reflecting strong electron-phonon coupling. Small penetration depths λ_o =125nm and large mean free paths $\ell \leq$ 15nm indicate high phase purity and accordingly weak quasiparticle scattering. A strong increase of microwave losses was observed at microwave field levels above B$_s \cong$ 15-25mT. The characteristic microwave parameters λ_o, j_c and B$_{s,on}$ depended on film thickness, and thus on grain size. These dependences reflect the influence of grain boundary scattering, pinning and microwave heating, respectively.

1. Introduction

Concerning high frequency applications of superconducting films, the understanding of the limiting mechanisms for the field dependent surface resistance $R_s(B_s)$ is still a challenging subject. For many superconductors a fundamental critical microwave field amplitude could not yet be determined. The distinction between intrinsic and extrinsic losses e. g., due to defects is often very difficult. Furthermore the intrinsic field limitation differs for type-I and type-II superconductors and depends on the values of e. g. coherence length ξ_o, mean free path ℓ, coupling strength, etc.

Nb$_3$Sn is an interesting material for comparative investigations with other low and also high temperature superconductors. Films on dielectric substrates allow to investigate the properties of the superconductor independently from possible interactions with a (super-) conducting substrate, and offer some advantages for planar microwave device applications.

In contrast to Nb$_3$Sn layers on bulk Nb, films on dielectric substrates were so far mainly prepared by magnetron sputtering [1] or electron-coevaporation [2]. High values of the residual resistance R$_{res}$ and penetration depth λ often reflected the presence of non-stoichiometric phases as well as of weak coupling across grain boundaries.

By combining two well-approved deposition techniques, we have prepared Nb$_3$Sn films on sapphire substrates, with properties comparable to those of Nb$_3$Sn layers on Nb-substrates [3]. This

process allows to controll the grain size. The effect of different grain size on the transport properties is described in the present work. We measured R_s at 87 and 19GHz for different temperatures and RF-(DC)-magnetic field amplitudes. Basic superconductor parameters such as the reduced gap Δ/kT_c, and λ_o were evaluated from the temperature dependent surface impedance. Mean free path, coherence lengh and London penetration depth λ_L were deduced from supplementary measurements of the temperature dependence of the upper critical field $B_{c2}(T)$ near T_c, as described in [4,5].

2. Preparation and structural properties

The two-step preparation process requires first the deposition of a Nb precursor film onto a sapphire substrate. This has been achieved by DC-magnetron sputtering. High sputtering rates of 1.5nm/s were applied in order to minimize oxygen gettering of the growing film. Typical film thickness were 0.1 - 3.0µm. In the second step, the Nb precursor was converted to Nb_3Sn by diffusion of tin vapour (TVD). The conversion was performed at temperatures of 1100-1200°C. Seperate heaters for the tin source and the sample allowed to adjust the tin vapour pressure independently of the sample temperature. This yielded optimum thermodynamic conditions for the formation of large-grained, phase-pure Nb_3Sn. As described in [6], the high, reproducible quality of the Nb_3Sn films was hardly affected by that of the Nb precursors.

Fig. 1 displays the SEM-images of the surfaces of three Nb_3Sn films with thickness d_{film} of 0.6µm (left), 1.2µm (middle), 2.1µm (right). The morphology with grain sizes in the micrometer range corresponds to that of Nb_3Sn on bulk Nb. The large grains are an advantage of the TVD-process, over one step processes where typical grain sizes stay in the nanometer range [1,7]. Obviously, the grain diameters and the film thickness are correlated and stay in the same range. This means that the two-step process offers the possibility to prepare films with adjusted grain sizes by converting differently thick Nb-precursors.
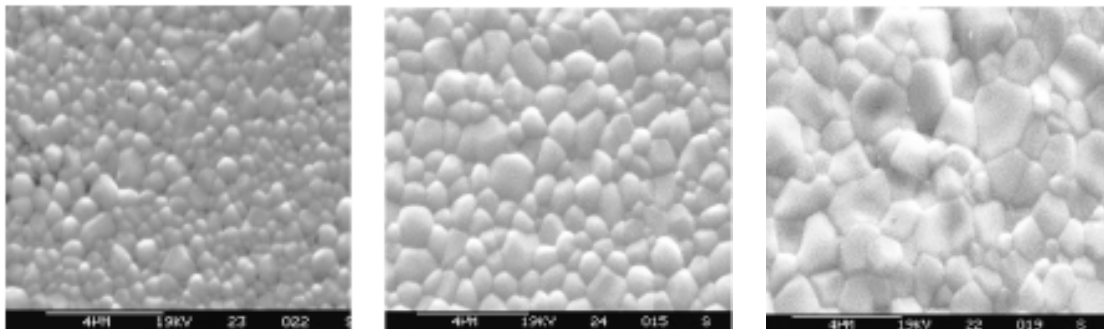

Fig. 1:
SEM pictures of three Nb_3Sn films: d_{film} = 0.6µm (left), 1.2µm (middle), 2.1µm (right).

3. Film thickness and transport properties

Fig. 2 displays typical temperature dependences of R_s and λ at 87GHz which are in accordance with the theoretical expectations. The measured data were corrected to the finite film thickness [8]. The measurements were carried out with a cylindrical Cu cavity, where the film replaced one endplate of the resonator [9]. The R_s(T)-curve show the transition to the superconducting state at T = 18.0K. At 4.2K, the surface resistance dropped below the sensitivity limit of 500µΩ. All features indicate high phase-purity of the films [2]. The measured R_s(T) and λ(T)-data were fitted to numerical

results calculated whithin the framework of the scaled BCS-theory [10]. Good agreement was achieved, with a reduced energy gap of $\Delta/kT_c = 1.8\text{-}2.3 \geq 1.76$ which indicate strong electron-phonon coupling. Deducing λ_o from the BCS-fit in the framework of the clean limit ($\xi_o << \ell$), the achieved values were systematicaly to small. Concerning thick films ($d_{film} \geq 1\mu m$) λ_o was in the range of 65-70nm. The $B_{c2}(T)$-measurements yielded $\xi_o \cong 9nm$ and $\ell \cong 15nm$ wich are relatively large in comparison with other published data [2,5] as well as $\lambda_L \cong 90nm$. Using these values the London penetration depth λ_L corresponded to a microwave penetration depth of $\lambda_o \cong 125nm$. That means that the λ_o values evaluated from the surface impedance data had to be shifted by an value of $\Delta\lambda \cong 55nm$.
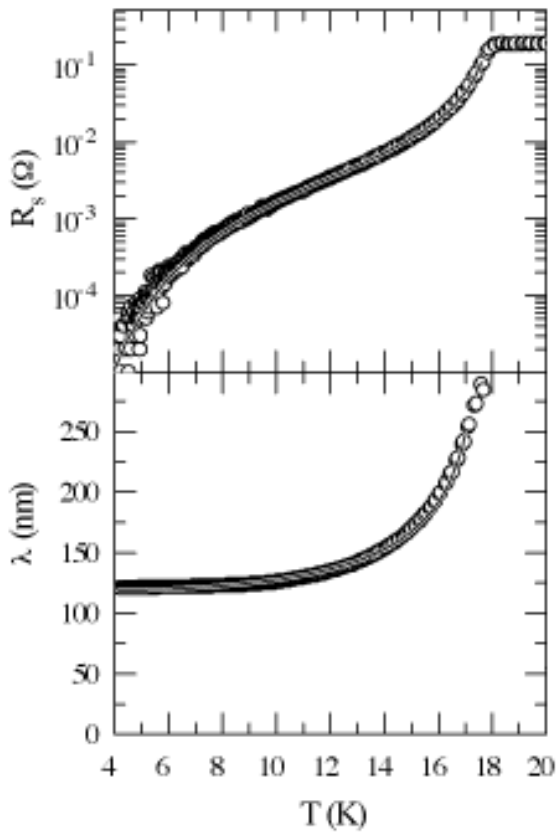

Fig. 2:
Comparison of measured (open circles) and calculated (solid lines) data of $R_s(T)$ and $\lambda(T)$ at 87 GHz for a typical TVD Nb_3Sn film on sapphire. A residual resistance of 500μΩ (resolution limit) was substracted from the R_s-data
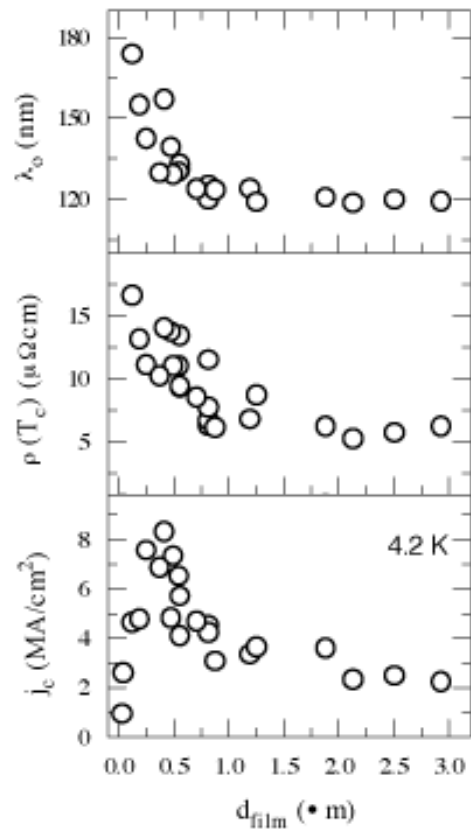
Fig. 3:
Comparison of the penetration pepth λ_o the normal conducting resistivity $\rho(T_c)$ and the current density j_c (42K) versus film thickness.

Fig. 3 compares the corrected penetration depth λ_o, the resistivity $\rho(T_c)$ (deduced from R_s according to the normal skin effect) and the critical current density j (4.2K) for film thicknesses up to 3.0μm. At $d_{film} \geq 1\mu m$, the low resistivity $\rho(T_c) \cong 7\mu\Omega cm$ reflects a high degree of ordering of the Nb chains

in the unit cells [11]. Reducing the film thickness d_{film}, $\rho(T_c)$ and λ_o start to increase monotonicaly. This reflects enhanced quasiparticle scattering, most likely due to an increased number of grain boundaries. The $j_c(4.2K)$ values also increase with decreasing d_{film} but reach a maximum at $d_{film} \cong$ 400nm, followed by a strong reduction for very thin films. Similar behavior was observed for Broze-processed Nb_3Sn filaments [12] and explained by enhanced pinning at grain boundaries (large thickness regime). In contrast at very small grain size weak link effects might become dominant and reduce j_c (low thickness regime).

4. Magnetic field dependence of the surface resistance

The microwave field dependent $R_s(B_s)$ was investigated at temperatures between 4.2K and 18K with 1″ diameter samples of different thickness. The measurements were performed in pulsed mode at 19GHz by using a Nb-shielded sapphire resonator [13] with a resolution limit of $20\mu\Omega$. Despite this high sensitivity R_{res} dropped below this limit. Due to the high Q-values ($5\cdot10^6$) typical pulse lengths are 400 - 600μs at pulse frequencies of 1Hz [13].

Fig. 4 displays two sets of $R_s(B_s)$ curves for different temperatures measured a) with a thick film (1.2μm) and b) with a thin film (250nm). The data points in Fig. 4a are figured up to field levels $B_{s,on}$ at which a sudden field breakdown occured as it is displayed for three different films in Fig. 5. Up to this values R_s increased by less than a factor 2. The following R_s-values, deduced from the pulse maximum increased further as indicated by the direction of the arrows. Absolute values of the breakdown levels $B_{s,on}$ at 4.2K were in the range of 15 - 25mT for d_{film} = 0.9 - 2.9μm. The temperature dependence of $B_{s,on}$ scaled like $1-(T/T_c)^4$ as expected for $1/\lambda^2$ in the two fluid model. This behavior was typical in most cases for all films with 0.9μm $\leq d_{film} \leq$ 2.9μm. The behavior observed for the thin film (Fig. 4b) was deviating and will be discussed in detail in section 4.3.
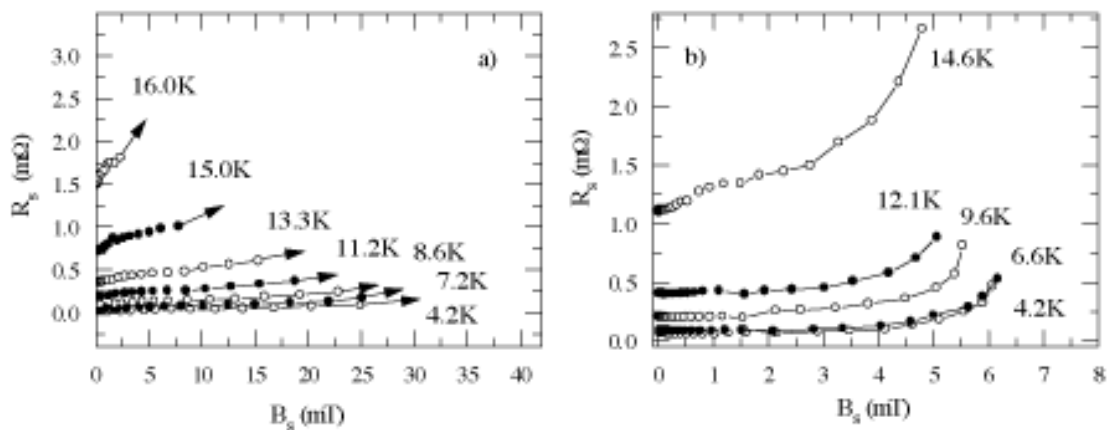

Fig. 4:
Microwave field dependence of the surface resistance R_s at 19GHz and different temperatures for two films with different thickness (1.2μm (a) and 250nm (b)). The arrows in a) indicate the field breakdown levels (see text).

4. 1. Comparison between RF- and DC-magnetic field

We have performed additional measurements of R_s in a superposed DC-magnetic field oriented perpendicular to the film surface. In Fig. 6, R_s as a function of B_s (solid symbols) is compared to R_s

measured at 87GHz as a function of the DC-field, (open symbols). In this case the $B_{s,on}$-value was 15mT. The DC-measurement yielded a significantly higher onset level around $B_{DC,on} \cong 50mT$, which allows to estimate a critical current density and the coresponding penetration field B_c^*. If the restricted power handling capability was solely limited by magnetic effects (e. g. pinning), $B_{s,on}$ should be comparable to B_c^*. At frequencies above the vortex nucleation frequency, dynamic superheating might occur, yielding even $B_{s,on} > B_c^*$. Thus, in any case $B_{s,on} \geq B_{DC,on}$ is expected. However this is in contrast with the experimental results. This discrepancy indicates that other mechanisms might dominate the power handling like, thermal limitations due to global or local heating.
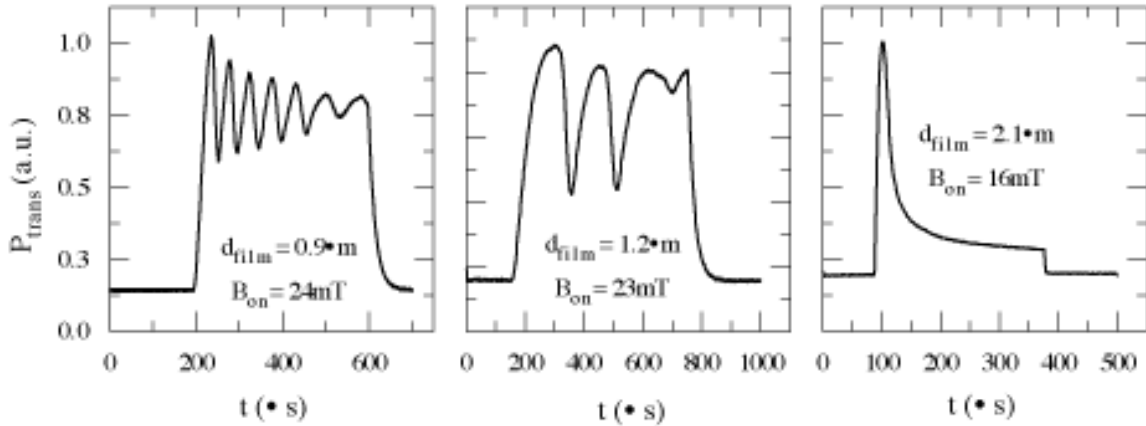

Fig. 5:
Different pulse shapes observed for three different films in the thickness range of 0.9μm to 2.1μm at the onset field level off additional losses at 4.2K.
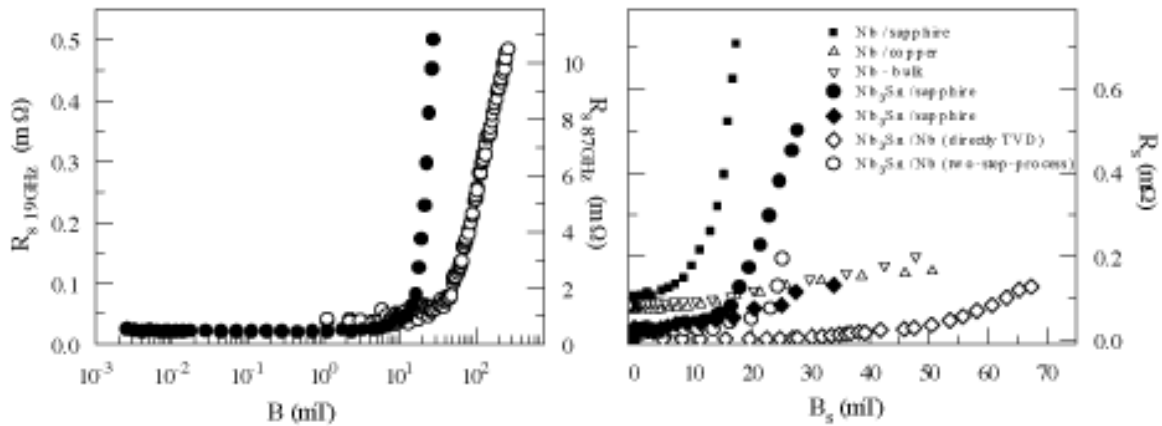

Fig. 6:
Magnetic field dependence of R_s at 19 GHz and 42 K for RF-(solid symbols,left y-axis) and at 87 GHz for DC-field (open symbols, right y-axis).

Fig. 7:
Coparison of $R_s(B_s)$-characteristics at 19 GHz of Nb_3Sn films on metal and sapphire substrates

4. 2. Evidence for thermal effects in thick films

Fig. 5 displays three different pulse shapes of the transmitted power observed for three different films, each at microwave field amplitudes slightly above $B_{s,on}$. It shows that the breakdown occurred with time constants of some 10-100μs, which is typical for thermal effects in the film or at the interface between film and substrate. Up to now all measurements yielded higher (lower) onset levels with the thinner (thicker) films. This correlation is in qualitative agreement with a simple thermal model based on local heating at defects, which yields $B_{s,on} \propto 1/d_{film}^{1/2}$ [14]. The different pulse deformations may reflect the different electrical and thermal properties of the relevant defects.

Fig. 7 compares $R_s(B_s)$ data of two Nb_3Sn films on sapphire- (solid symbols) with two films on Nb-substrates (open symbols). One of the latter stands for a film deposited by the two-step-process onto a polished Nb-disc (open circles; sample A). The other data (open diamonds; sample B) were deduced from frequency-scaled ($R_s \propto f^2$) data of a Nb_3Sn film prepared by TVD on a Nb-cavity at 1.5GHz [3]. Sample B showed a smaller increase of R_s with increasing B_s than the similar prepared films on sapphire. The $R_s(B_s)$-data from sample A look similar to the best results achieved with films on sapphire. Considering the rather similar low-field properties of the films on sapphire and bulk Nb, the differences concerning the RF-field dependences might be affected by the substrate material. This assumption is supported by $R_s(B_s)$-data obtained with Nb films on metallic and dieletric substrates [13]. These are shown in Fig. 7 by the small symbols: Nb film on sapphire (solid squares), on Cu (open triangles) and Nb-bulk (open triangles, upside down). The two metallic samples Nb/Nb and Nb/Cu showed comparable field dependences of R_s. In contrast, the metal/dielectric sandwich Nb/sapphire showed enhanced nonlinearities which resemble those of Nb_3Sn/sapphire in comparison with Nb_3Sn/Nb. These results may be indicative of different substrate-induced film growth with different microstructures and/or morphologies as known for Nb/sapphire [15], and suspected for Nb/Cu [16]. Another possible source for the different $R_s(B_s)$-dependences is the thermal boundary resistance of the film-substrate-interface. The more strongly this interface hinders the heat transport from the film surface to the cold sink, the stronger heating of the film is expected with the consequence of increasing surface impedance. This may also explain the differences between the two Nb_3Sn films on Nb. It is obvious that the different preparation processes (i.e. two-step-process vs. directly TVD) will affect the transport properties of the interfaces.

4. 3. $R_s(B_s)$ of thin films

$R_s(B_s)$-behavior deviating from that described for the thick films was observed for the thin film ($d_{film} = 250$ nm) as displayed in Fig. 4b. No sudden field breakdown was observed, but a continuous degradation of R_s which allowed only to reach a field level of 6 mT at 4.2K. The time constant of the nonlinearity was much smaller in this case than those observed before. It is presently not clear whether this behavior can also be understood thermal in origin. Alternatively, the small film thickness and the correspondingly large density of grain boundaries could induce granular $R_s(B_s)$ behavior. That would mean that there is an analogous crossover for $R_s(B_s)$ as for j_c defined by the grain size. Thermal effects clearly dominate $R_s(B_s)$ in large-grained films. In contrast, granularity might be dominant in fine-grained films. Further investigations are in progress for a better understanding of these mechanisms.

5. Summary

The two-step-process of sputtering Nb precursor films and converting them by diffusion of Sn-vapour allows the deposition of phase-pure, large-grained Nb Sn films onto sapphire substrates. The transport properties were comparable to Nb_3Sn layers on bulk Nb prepared by TVD. These technique offers the possibility to vary the grain size by converting Nb precursors of different thickness. Systematic investigations showed a clear influence of the grain structure on the transport parameters. Variations of the quasiparticle scattering, pinning and weak link properties were observed. In microwave fields R_s(19GHz, 4.2K) stayed constant only up to 15 - 25mT. In superposed DC-magnetic field, R_s(87GHz, 4.2K) increased above 50mT yielding no clear evidence for magnetic limitations.Time resolved measurements of $R_s(B_s)$ of thick films hinted for thermal limitations (time constants $\leq$ some 100µs). The comparison of Nb_3Sn and Nb films on sapphire and metal substrates indicated an influence of the substrate material and/or the substrate film interface on the $R_s(B_s)$-dependence. With films on dielectric substrates, lower onset levels were observed.

Acknowledgements

References

[1]   Andreone A et al. 1997 *IEEE Trans. Appl. Supercond.* **Vol. 7 No. 2** 1772

[2]   Allen L H, Beasley M R, Hammond R H, Turneaure J P 1987 *IEEE Trans. Magn.* **MAG-23** 1405

[3]   Müller G et al. 1996 *Proc. 5th Europ. Part. Acc. Conf.. EPAC 96 Sitges* **Vol. 3** 2085

[4]   Mahner E 1989 *University of Wuppertal Germany* report WUD 89-13

[5]   Orlando T P, McNiff E J, Foner S, Beasley M R 1979 *Phys. Rev B* **Vol. 19 No. 9** 4545

[6]   Perpeet M et al. 1997 *J. Appl. Phys.* **82** (9)

[7]   Wu C T , Kampwirth R T, Hafstrom J T 1977 *J. V . Sic. Technol.* **Vol. 14** 134

[8]   Klein N et al. 1989 *Appl. Phys. Lett.* **54** 757

[9]   Hensen S et al. 1993 in *Appl. Supercond.(DGM, Oberursel).* 1053

[10]   Halbritter J 1969 *PhD-thesis Forschungszentrum Karlsruhe Germany* report 3/69-2

[11]   Flükiger R et al. 1987 *IEEE Trans. Magn.* **MAG-23** 980

[12]   Suenaga M *Superconductor Materials Science: Metallurgy, Fabrication and Applications,* edited by S. Foner and B. B. Schwartz (Plenum, New York, 1981)

[13]   Th. Kaiser et al. *This Conference*

[14]   Hein M A 1998 *University of Wuppertal Germany* to be published

[15]   Srolovitz D J 1986 *J. Vac. Sci. Technol.* **A4** 2925

[16]   Bloess D et al. 1997 *IEEE Trans. Appl. Supercond.* **Vol. 7 No. 2** 1776